

# Verification of Lossless ZVS Condition for Three-Phase AC-DC CIHRC

Rahimi Baharom, Mohammad Nawawi Seroji, and Ahmad Ihsan Mohd Yassin  
 Faculty of Electrical Engineering, Universiti Teknologi MARA, 40450 Shah Alam, Selangor, Malaysia.  
 Email: rahimi6579@gmail.com

**Abstract**—This paper presents the verification of lossless zero voltage switching (ZVS) condition for three-phase AC to DC current injection hybrid resonant converter (CIHRC). Details on the operation of current injection technique with ZVS condition on shaping the sinusoidal and continuous supply current waveforms are presented. With an appropriate design of hybrid resonant circuit and a suitable switching frequency selection, the device is capable to operate under virtually lossless ZVS conditions allowing reduction in the size of inductive and magnetic components with high frequency operation. Selected simulation results are also presented to verify the lossless ZVS condition for three-phase AC-DC CIHRC.

**Index Terms**—AC-DC converter, current injection, hybrid resonant converter, zero voltage switching (ZVS).

## I. INTRODUCTION

Rectifier or AC-DC conversion can be performed using a single diode which will allow the current to flow in a single direction. Enhancing the circuit by adding and arranging more diodes will form the half-bridge and full-bridge configurations resulting in an improved output voltage ripple level and thereby its efficiency as well. Due to the merits such as low switch stress, low output ripple and better power factor, the three-phase converter variants were preferred as compared to the single-phase variants [1]. Basically, the three-phase AC-DC converter circuit utilizes the bridge diode rectifier to perform their operations in half-bridge or half-wave and full-bridge or full-wave mode. The half-bridge three-phase rectifier utilizes three diodes to convert an AC voltage into a unidirectional form. Full-bridge configuration that employs six diodes has been developed to improve the output voltage ripple in order to eliminate the 3<sup>rd</sup> harmonics that could result in an improved total harmonic distortion (THD) level. Because of this, the three-phase AC-DC converter circuit utilizes the full-bridge diode rectifier to perform their operations attributed by advantages such as low cost, simple and reliable structure, high efficiency, and low electromagnetic interference noise [2]. Unfortunately, highly distorted input current waveforms are generated using this topology. This would cause potential problems such as low overall Power Factor (PF) ( $PF = \text{real power} \div \text{apparent power}$ ), heating effects, device malfunction and destruction of other equipment caused

by non-linear load [3]-[12]. Moreover, additional harmonic losses in the utility system would excite the electrical resonance, leading to high over-voltages [13].

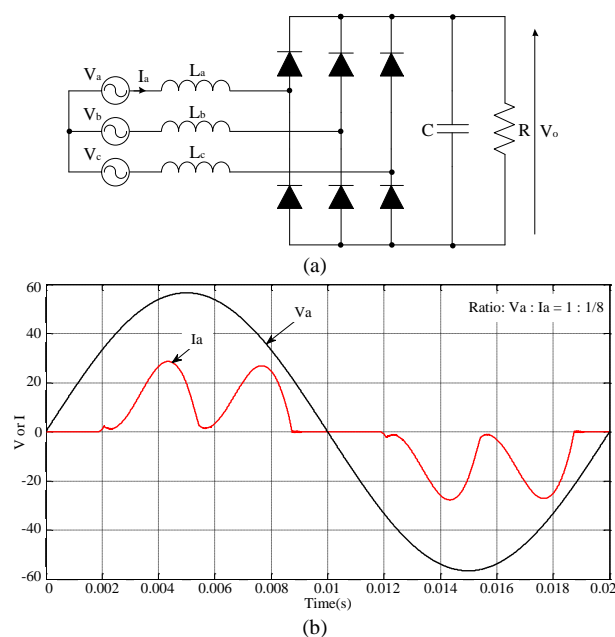


Figure 1. Conventional diode bridge three-phase AC-DC converter (a) Circuit configuration, (b) Associated line current and voltage waveform.

Conventional three-phase AC-DC converter circuit as shown in Fig. 1 (a) used diode-bridge to perform their operations due to the attractive characteristics such as low cost, simple and reliable structure, high efficiency, and low electromagnetic interference noise [14]. However, it will produce undesirable distorted line current as shown in Fig. 1 (b) with low power factors which could possibly cause harmonic pollution in the power supply system [13] [14]-[17]. Thus, in order to avoid the harmonic pollution of the utility system, several standards such as the IEEE Std. 519 have been developed and were being enforced on the harmonic content of the current and voltage drawn by power electronic converters [1], [15], [17]. To solve this problem, other options such as power factor correction (PFC) converters and active power filter technique to compensate for the harmonic current generated by the diode rectifiers have been developed extensively [14].

In light of the strict requirement of power quality at input AC mains, several three-phase power factor

correction for AC-DC converter have been proposed [18]. The three-phase AC-DC converters have been developed these days to a matured level with improved power quality in terms of power-factor correction, reduced total harmonic distortion at input AC mains, regulated DC output and in compliance with standards concerned [8], [19].

To achieve this goal, the PFCs functions were usually used in order to obtain high efficiency of the electric energy conversion. However, most of the conventional PFCs systems employed pulse width modulation (PWM) techniques to achieve the features of the PFCs function converters [6], [20], [21]. Recently, with the increasingly grown interest to have more compact power supply encouraged higher operating frequencies causing the PWM converters to fall short. This is because at such high frequency operation, the parasitic elements established enormous stress on the circuit elements associated with a noticeable electromagnetic interference (EMI) emission [22]. In addition, the use of hard switching technique consisted of delay/decay time for its current or voltage to fully turn-ON or OFF a switch resulting in switching loss that is proportional to the increase in the switching frequency.

The resonant converters are known to have distinct advantages like higher efficiency, higher power density, reduced EMI and lower component stresses over the hard-switching PWM converters have been found to be a good solution to the above mentioned problem [23]. Due to the virtual elimination of the switching losses or stress in the power switches using the natural commutation of the resonant converter, the operating frequency of the resonant converter could be high resulting in small values for the magnetic and inductive components such as resonant inductors and transformers thus improving the power density of the power supply system [24]. The main idea behind the use of resonant converters was to provide soft switching transitions through an appropriate design of resonant circuit and switching frequency selection which enables the devices to operate virtually under lossless Zero Current Switching (ZCS) or Zero Voltage Switching (ZVS) conditions. Hence, it was possible to achieve higher switching frequency operation.

II. SWITCHING CONDITION OF LOADED RESONANT POWER CONVERTER

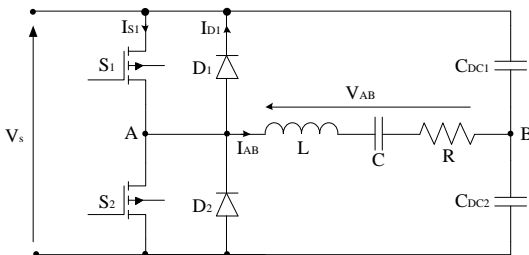


Figure 2. Half-bridge and series L-C-R network.

In principle, the switching condition in a resonant converter can be divided into two conditions namely; switching frequency below resonance frequency and switching frequency above the resonance frequency. A

resonant converter operation achieves their resonance condition when the magnitude of both inductive and capacitive reactance was equal but cancels each other because they were 180 degree in phase [25]. In order to understand these conditions, a basic half-bridge resonant circuit with series L-C-R network as shown in Fig. 2 was used. Then, the related waveform such as voltages and currents are sketched as shown in Fig. 3 and Fig. 4 to illustrate the switching conditions for both the switching frequency below and above resonant frequencies.

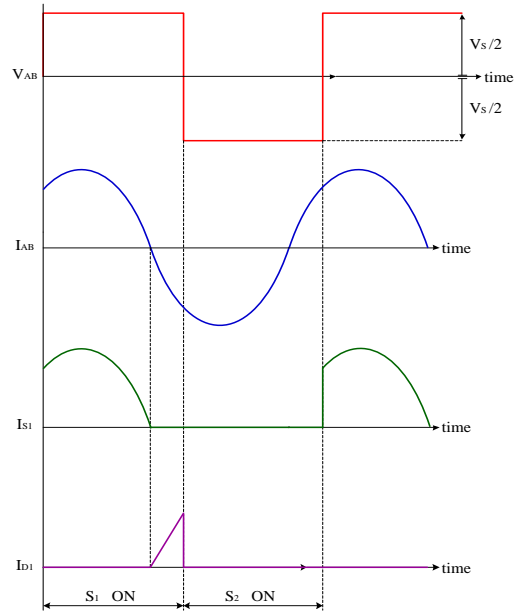


Figure 3. Half-bridge and L-C-R network waveforms for switching frequencies slightly below the resonant frequency.

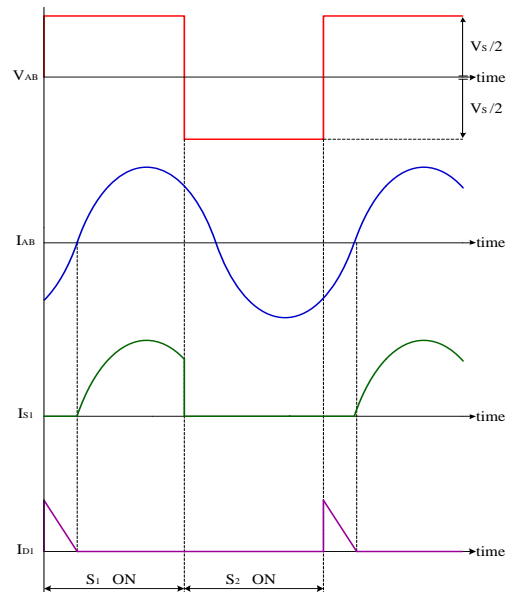


Figure 4. Half-bridge and L-C-R network waveforms for switching frequencies slightly above the resonant frequency.

A. Switching Frequency Below Resonant Frequency

The switching frequency operation below the natural resonant frequency is also called leading power factor mode of operation. This phenomenon is illustrated in Fig.

3 where it shows that the current  $I_{AB}$  leads the voltage  $V_{AB}$ .

The converter can operate in two modes of operation which are continuous and discontinuous current modes [26]. The discontinuous conduction mode occurs when the switching frequency operation is less than 50% of the resonant frequency. When the switching frequency operation was between 50% and 100% of the resonant frequency, the continuous conduction mode will occur [25]. The output voltage of the converter can be regulated by decreasing the switching frequency operation below the rated value [26].

By referring to Fig. 3, for the switching frequency below the resonant frequency, the diode was conducted resulting in the switch current,  $I_{S1}$  being brought to zero before the gate voltage was removed. During this time, the turn-OFF transition occurred when the current is zero, thus obtaining the ZCS. However, there were several disadvantages were identified for operation with the below resonance mode. Additional snubber inductors were required to reduce the large turn-ON switch currents besides the need for fast recovery diodes. In addition, by decreasing the switching frequency operation below the rated value to control the output voltage of the converter could lead to designing the high-frequency transformer and magnetics at the lowest switching frequency. As a result, the size of the converter also increased [26].

**B. Switching Frequency Above Resonant Frequency**

The switching frequency above the resonant frequency is also called lagging power factor mode of operation. The typical operating waveform of switching frequency above resonant frequency as shown in Fig. 4, clearly shows that the current  $I_{AB}$  lagged the voltage  $V_{AB}$ .

By referring to the waveform for the half-bridge and L-C-R network as shown in Fig. 2, the intrinsic body diode of a MOSFET was used to allow the current,  $I_{D1}$  to flow from the source to drain. The current flow through the body diode will clamp the voltage across the switch to a negligible voltage level so that the turn-ON switching losses were significantly reduced. Therefore, by forcing the switch voltage to zero before the switch current flowing through it will obtain the ZVS. For the switching frequency operation above resonance, only a simple snubber capacitor was required by removing the  $di/dt$  limiting inductance used during the switching frequency operation below resonant frequency. This occurs due to the switch of the resonant converter taking the current from its own diode across it at zero-current point [26]. Thus, the turn-OFF losses of the switch could also be virtually eliminated by the use of capacitive snubbers [27].

**III. ZERO VOLTAGE SWITCHING OPERATION**

The existing topology of the three-phase AC-DC converter with improved power factor and output voltage regulation using high frequency current injection technique was used and applied in series resonant circuit configuration [29]. Due to setbacks of the existing circuit topology like being limited to regulate the output voltage

at light or zero load conditions, the three-phase AC-DC CIHRC was developed [30]-[32]. The principle features of the proposed three-phase AC-DC CIHRC include continuous current operations of three AC supply currents, inherent shaping of the supply currents resulting in high power factor and low total harmonic distortion (THD) level employing only two soft-switched active devices.

The circuit structure of the three-phase AC-DC CIHRC is presented in the Fig. 5 which consists of a single, high-frequency inverter leg that operates from the split-capacitor DC-link where the transistor duty ratios were fixed at 0.5. The autotransformer  $T_A$  steps up the output voltage from the switching leg and drove a sinusoidal current through the hybrid resonant circuit. The resonant current was rectified to form the output and was also injected into the three-phase utility-frequency rectifier to modulate the rectifier input voltages resulting in continuous and sinusoidal line currents. The inclusion of capacitor  $C_{PA}$  at the input of the high frequency full-wave rectifier is the main difference with the series circuit topology, thus, make this circuit topology operate as hybrid resonant converter. An appropriate design of the resonant circuit and switching frequency selection enabled the devices to operate virtually under lossless zero voltage switching (ZVS) conditions.

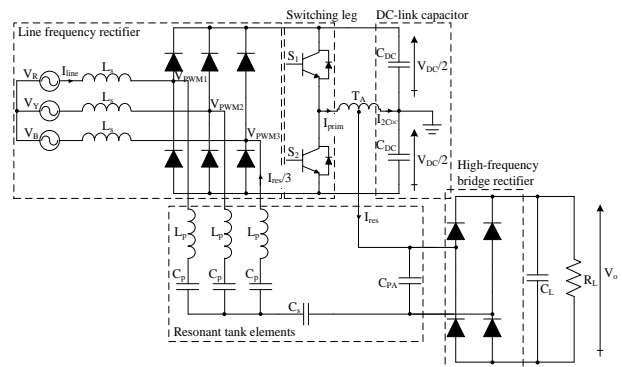


Figure 5. The three-phase AC-DC current injection hybrid resonant converter topology

In order to understand the three-phase AC-DC CIHRC better, the single leg of this circuit topology is illustrated in Fig. 6 (a).  $V_s$  represents one of the phase voltages supplied by the connected configuration. The resonant current  $I_{res3}$  is considered as 1/3 of the converter resonant current  $I_{res}$  and was injected into the mid-point of the diode leg. The resulting modulation of the diode midpoint voltage  $V_{PWM}$  was modulated by a process of summation of the sinusoidal supply current  $I_{line}$  and the resonant current  $I_{res3}$ . When the sum of the sinusoidal supply current  $I_{line}$  and the resonant current  $I_{res3}$  is greater than zero, the upper diode of the three-phase diode bridge rectifier conducts resulting in  $V_{PWM}$  equals to  $+V_{DC}/2$ . Meanwhile, the lower diode conducts when the sum of the sinusoidal supply current  $I_{line}$  and the resonant current  $I_{res3}$  is less than zero resulting in  $V_{PWM}$  becoming  $-V_{DC}/2$ . Fig. 6 (b) shows the fundamental frequency equivalent circuit for the half-bridge hybrid resonant converter. Through this technique, the line current  $I_{line}$ , will sustain the sinusoidal current waveform.

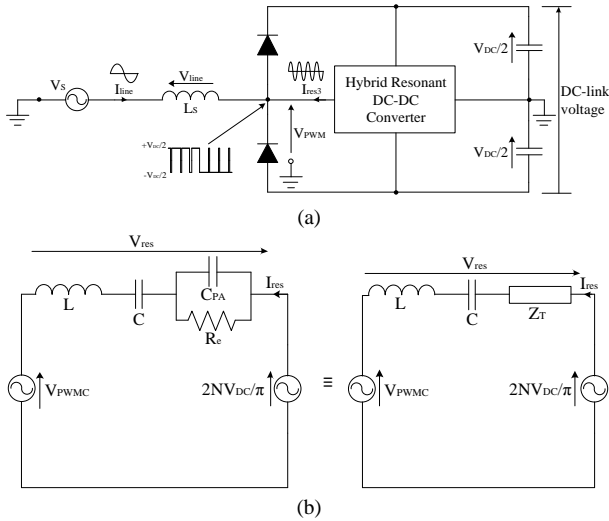


Figure 6. (a) Single leg of converter fed by hybrid resonant converter, (b) Fundamental frequency equivalent circuit for the half-bridge hybrid resonant converter.

The steady-state analysis could be derived based on the fundamental frequency equivalent circuit to determine the parameters of the proposed converter. The total impedance of  $Z_T$  is defined as the equivalent parallel connection of the Steigerwald equivalent input resistance  $R_e = \pi^2 R / 8$  [28], with the capacitor  $C_{PA}$  which is the main difference with the series circuit configuration. Based on Fig. 6 (b), the hybrid configuration of the resonant converter was produced by splitting the resonant capacitor into two components,  $C$  and  $C_{PA}$  with the load connected with  $C_{PA}$  in the parallel configuration. The fundamental voltage at the output of the switching leg autotransformer is represented by  $2NV_{DC}/\pi$ , where  $N$  being the autotransformer voltage step up ratio [28].

At heavy-load conditions, the parallel capacitor  $C_{PA}$  was effectively shorted by a relatively low input resistance of rectifier circuit. In this condition, the

operation of the resonant tank was dominated by  $L$  and  $C$  and the converter took on the characteristics of a series loaded converter. At light-load conditions meanwhile, the parallel capacitor  $C_{PA}$ , was no longer effectively shorted since the rectifier input resistance had increased. In this condition therefore, the converter took on the characteristics of a parallel loaded converter. As a result, by using the hybrid loaded configuration, the output voltage can be regulated at light and zero load conditions.

#### IV. COMPUTER SIMULATION MODEL

The MATLAB/Simulink simulation circuit of the three-phase AC-DC CIHRC is shown in Fig. 7. The parameters of the DC link capacitor  $C_{DC}$  was obtained by estimating that the peak current flow through the capacitors  $C_{DC1}$  and  $C_{DC2}$  was the difference between the primary and secondary currents of the autotransformer. Details parameters for the simulation model of three-phase AC-DC CIHRC have been discussed in [30]-[32].

Fig. 8 shows the red phase supply current waveform while Fig. 9 shows the combination of the red phase supply current with the supply voltage waveforms where the peak line current was 12.6 A and the peak supply voltage of 57 V. The result shows that the supply current is continuous, sinusoidal and in-phase with the supply voltage resulting in low total harmonic distortion (THD) level of 3.11% with the high input displacement power factor of 0.997. Table I shows the comparison of the magnitude of the individual harmonics for the supply current waveform with IEEE Std. 519. The amplitude of the low order harmonics such as 5<sup>th</sup>, 7<sup>th</sup>, 9<sup>th</sup>, 11<sup>th</sup>, 13<sup>th</sup>, and 15<sup>th</sup> are below the percent of maximum values that was defined by the IEEE Std. 519, thus, the result shows that the THD level of the supply current for the converter is well below the acceptable limit that is defined and meets the IEEE Std. 519.

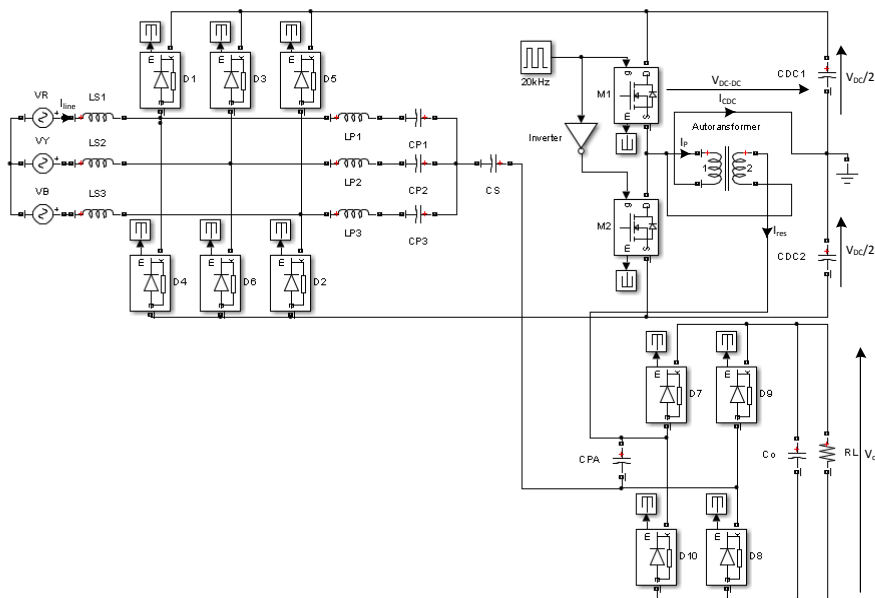


Figure 7. Simulation model of CIHRC in MATLAB/Simulink.

TABLE I: IEEE STD. 519 STANDARD LIMITS, HARMONICS OF PHASE CURRENT, POWER FACTOR AND THD

Harmonics order	IEEE Std. 519 (%)	Simulation (%)
5 <sup>th</sup>	4	1.28
7 <sup>th</sup>	4	0.96
9 <sup>th</sup>	4	0
11 <sup>th</sup>	2	1.32
13 <sup>th</sup>	2	0.31
15 <sup>th</sup>	2	0
THD (%)		3.11
P.F		0.997

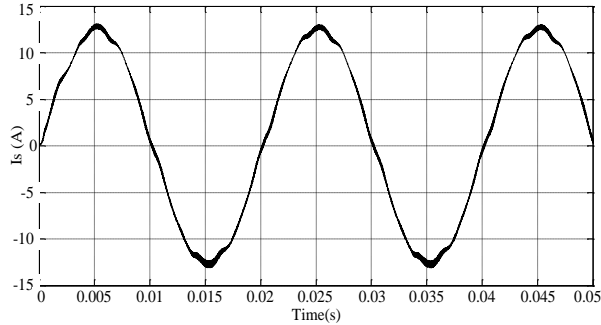


Figure 8. Simulation result of red phase supply current waveform of CIHRC in MATLAB/Simulink.

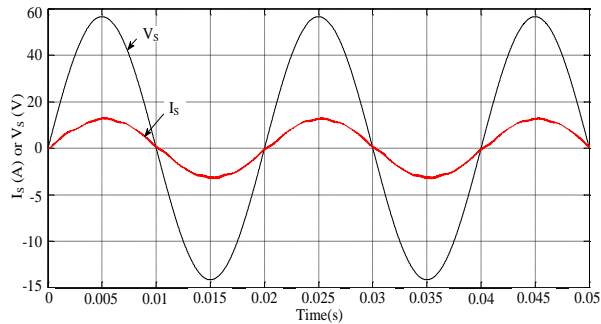


Figure 9. Simulation result of supply current and voltage waveforms of CIHRC in MATLAB/Simulink.

The estimated efficiency of the proposed converter is calculated based on the equations as follows:

$$\eta = \frac{P_{out}}{P_{in}} = \frac{V_o^2 / R_L}{3V_s I_{line} \cos \phi} \quad (1)$$

Thus, the efficiency of the converter can be determined using (1), resulting in  $\eta$  is 95%. The power factor, PF of the proposed converter can be determined as

$$PF = df \psi \quad (2)$$

where  $df$  is the displacement power factor (displacement angle between the input voltage and input current,  $\cos \phi = 0.997$ ) and  $\psi$  is the distortion factor that can be determine as [25]:

$$\psi = \sqrt{\frac{1}{THD^2 + 1}} \quad (3)$$

From the simulation result of THD of 0.0311, the  $\psi$  is equal to 0.9995. Thus, by solving (2) and (3), the power factor of the converter of 0.997 was obtained.

The converter resonant current  $I_{res}$  waveform and switching leg voltage  $V_{DC-DC}$  waveform are shown in Fig.

10. The converter resonant current  $I_{res}$  was approximately sinusoidal with a peak value of 34 A. Based on Fig. 10, it was observed that the resonant current lagged behind the switching leg voltage by an angle of  $-20.44^\circ$  in order to perform the zero voltage switching operation. Fig. 11 shows the simulation result of the upper switch (S1) and lower switch with PWM signal during positive and negative cycle operations respectively. Based on Fig. 11, when the lower switch is turned-OFF, the resonant current cannot flow through the lower switch. Hence, the only path that the resonant current has is through the body diode of the upper switch which is illustrated by the negative current of  $I_s$ , results in the voltage across the upper switch  $V_{DS}$  equals to zero. It can be observed that both switches perform their zero-voltage-switching, thus verified the soft switching transitions of the converter. Fig. 11 illustrates that the MOSFET operates with zero-voltage-switching, however due to the tail current, turn-OFF losses were excessive and this was the dominant factor which affected the converter efficiency.

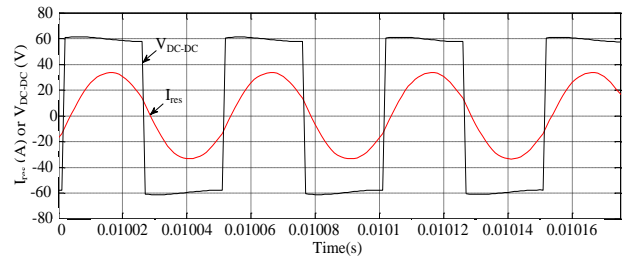
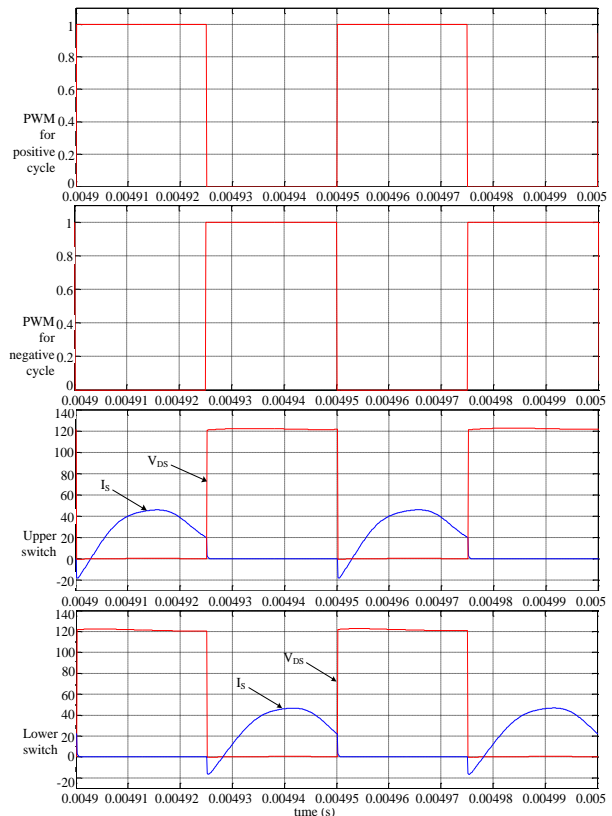

 Figure 10. Simulation result of resonant current  $I_{res}$  and switching leg voltage  $V_{DC-DC}$  waveforms of CIHRC in MATLAB/Simulink.


Figure 11. Simulation result of supply current and voltage waveforms of CIHRC in MATLAB/Simulink.

## V. CONCLUSION

In this paper, verification of the lossless ZVS condition for the three-phase AC-DC CIHRC was presented. The implemented simulation models was developed using MATLAB/Simulink. The performance of the converter has been evaluated by assessing the efficiency, the power factor and the total harmonic distortion (THD). The comparison of the individual harmonic spectrum of the red phase supply current waveform with the IEEE Std 519 showed that all of the harmonic spectrum were well below the acceptable limit and satisfied the standard.

## ACKNOWLEDGMENT

Authors gratefully acknowledge the financial support from Institute of Research Management and Innovation (IRMI) Universiti Teknologi MARA Grant No: 600-IRMI/MyRA 5/3/BESTARI (029/2017).

## REFERENCES

- [1] J. Shah and G. Moschopoulos, "Three-phase rectifiers with power factor correction," in *Proc. Canadian Conf. on Electrical and Computer Engineering*, May 2005, pp. 1270-1273.
- [2] W. Jiang, S. Xu, N. Li, Z. Lin, and B. W. Williams, "Wireless power charger for light electric vehicles," in *Proc. of IEEE 11<sup>th</sup> Int. Conf. on Power Electronics and Drive Systems*, June 2015, pp. 562-566.
- [3] D. S. Wijeratne and G. Moschopoulos, "A comparative study of two buck-type three-phase single-stage AC-DC full-bridge converters," *IEEE Trans. on Power Electronics*, vol. 29, no. 4, pp. 1632-1645, April 2014.
- [4] S. C. Shin, H. J. Lee, Y. H. Kim, J. H. Lee, and C. Y. Won, "Transient response improvement at startup of a three-phase AC/DC converter for a DC distribution system in commercial facilities," *IEEE Trans. on Power Electronics*, vol. 29, no. 12, pp. 6742-6753, Dec. 2014.
- [5] S. A. Saleh and M. A. Rahman, "Optimal resolution level for input-output control of 3 $\phi$  VSPWM AC-DC converters," *IEEE Trans. on Industry Applications*, vol. 50, no. 2, pp. 1432-1447, March 2014.
- [6] M. Narimani and G. Moschopoulos, "A new interleaved three-phase single-stage PFC AC-DC converter," *IEEE Trans. on Industrial Electronics*, vol. 61, no. 2, pp. 648-654, Feb. 2014.
- [7] Y. Zhang, W. Xie, and Y. Zhang, "Deadbeat direct power control of three-phase pulse-width modulation rectifiers," *IET Power Electronics*, vol. 7, no. 6, pp. 1340-1346, June 2014.
- [8] K. You, D. Xiao, M. F. Rahman, and M. N. Uddin, "Applying reduced general direct space vector modulation approach of AC-AC matrix converter theory to achieve direct power factor controlled three-phase AC-DC matrix rectifier," *IEEE Trans. on Industry Applications*, vol. 50, no. 3, pp. 2243-2257, May 2014.
- [9] D. S. Wijeratne and G. Moschopoulos, "A novel three-phase buck-boost AC-DC converter," *IEEE Trans. on Power Electronics*, vol. 29, no. 3, pp. 1331-1343, March 2014.
- [10] M. Alam, W. Eberle, D. S. Gautam, C. Botting, N. Dohmeier, and F. Musavi, "A hybrid resonant pulse-width modulation bridgeless AC-DC power factor correction converter," *IEEE Trans. on Industry Applications*, vol. 53, no. 2, pp. 1406-1415, 2017.
- [11] B. Poorali, E. Adib, and H. Farzanehfar, "A single-stage single-switch soft-switching power-factor-correction LED driver," *IEEE Trans. on Power Electronics*, vol. 32, no. 10, pp. 7932-7940, 2017.
- [12] J. Kim, S. Lee, W. Cha, and B. Kwon, "High-Efficiency bridgeless three-level power factor correction rectifier," *IEEE Trans. on Industrial Electronics*, vol. 64, no. 2, pp. 1130-1136, 2017.
- [13] D. Alexa, A. Sirbu, D. M. Dobrea, and T. Goras, "Topologies of three-phase rectifiers with near sinusoidal input currents," *IEE Proc. - Electric Power Applications*, vol. 151, no. 6, pp. 673-678, Nov. 2004.
- [14] H. Wang, M. Su, Y. Sun, J. Yang, G. Zhang, W. Gui, and J. Feng, "Two-stage matrix converter based on third-harmonic injection technique," *IEEE Trans. on Power Electronics*, vol. 31, no. 1, pp. 533-547, Jan. 2016.
- [15] J. C. Pelicer, F. J. M. de Seixas, A. C. de Loureno, and L. de S. da C. e Silva, "Novel isolated multi-pulse rectifiers with low current distortion using three-phase half-controlled boost converters," in *Proc. IEEE 13<sup>th</sup> Brazilian Power Electronics Conference and 1<sup>st</sup> Southern Power Electronics Conference*, Nov. 2015, pp. 1-5.
- [16] C. Rech and J. R. Pinheiro, "Line current harmonics reduction in multi-pulse connection of asymmetrically loaded rectifiers," *IEEE Trans. on Industrial Electronics*, vol. 52, no. 3, pp. 640-652, June 2005.
- [17] B. Singh, V. Garg, and G. Bhuvaneswari, "Polygon-connected autotransformer-based 24-pulse AC-DC converter for vector-controlled induction-motor drives," *IEEE Trans. on Industrial Electronics*, vol. 55, no. 1, pp. 197-208, Jan. 2008.
- [18] H. Mao, C. Y. Lee, D. Boroyevich, and S. Hiti, "Review of high-performance three-phase power-factor correction circuits," *IEEE Trans. on Industrial Electronics*, vol. 44, no. 4, pp. 437-446, Aug. 1997.
- [19] B. Singh, B. N. Singh, A. Chandra, K. Al-Haddad, A. Pandey, and D. P. Kothari, "A review of three-phase improved power quality AC-DC converters," *IEEE Trans. on Industrial Electronics*, vol. 51, no. 3, pp. 641-660, June 2004.
- [20] T. Friedli, M. Hartmann, and J. W. Kolar, "The essence of three-phase PFC rectifier systems-Part II," *IEEE Trans. on Power Electronics*, vol. 29, no. 2, pp. 543-560, Feb. 2014.
- [21] J. W. Kolar and T. Friedli, "The essence of three-phase PFC rectifier systems-2014; Part I," *IEEE Trans. on Power Electronics*, vol. 28, no. 1, pp. 176-198, Jan. 2013.
- [22] M. Z. Youssef and P. K. Jain, "A novel single stage AC-DC self-oscillating series-parallel resonant converter," *IEEE Trans. on Power Electronics*, vol. 21, no. 6, pp. 1735-1744, Nov. 2006.
- [23] Z. Ye, J. C. W. Lam, P. K. Jain, and P. C. Sen, "A robust one-cycle controlled full-bridge series-parallel resonant inverter for a high-frequency AC (HFAC) distribution system," *IEEE Trans. on Power Electronics*, vol. 22, no. 6, pp. 2331-2343, Nov. 2007.
- [24] S. Morrison, "Analysis of a hybrid series parallel resonant bridge converter," *IEEE Trans. on Power Electronics*, vol. 7, no. 1, pp. 119-127, Jan. 1992.
- [25] A. B. Basri, N. A. Zaidi, N. B. Bopi, E. H. Aboadla, S. Khan, and M. H. Habaebi, "Effects of switching frequency to series loaded series resonant circuit," *ARPN Journal of Engineering and Applied Sciences*, vol. 11, no. 1, pp. 382-386, January 2016.
- [26] R. C. Dorf, Ed., *Electronics, Power Electronics, Optoelectronics, Microwaves, Electromagnetics, and Radar*, CRC Press, 2006.
- [27] S. V. M. A Cross and A. J. Forsyth, *High Frequency Power Electronic Circuits and Systems*, School of Electronic & Electrical Engineering, The University of Birmingham, 1998.
- [28] A. M. Cross and A. J. Forsyth, "A high-power-factor, three-phase isolated AC-DC converter using high-frequency current injection," *IEEE Trans. on Power Electronics*, vol. 18, no. 4, pp. 1012-1019, July 2003.
- [29] M. N. Seroji and A. J. Forsyth, "Small-signal model of a high-power-factor, three-phase AC-DC converter with high-frequency resonant current injection," in *Proc. Int. Conf. on Power Electronics and Drives Systems*, 2005, pp. 462-467.
- [30] R. Baharom, M. N. Seroji, and M. K. M. Salleh, "Computer simulation model and performance analysis of high power factor three-phase AC-DC current injection hybrid resonant converter," in *Proc. IEEE 10<sup>th</sup> Conf. on Industrial Electronics and Applications*, 2015, pp. 1403-1407.
- [31] R. Baharom, M. N. Seroji, M. K. M. Salleh, and K. S. Muhammad, "A high power factor three-phase AC-DC current injection hybrid resonant converter," in *Proc. 42<sup>nd</sup> Annual Conf. of the IEEE Industrial Electronics Society*, 2016, pp. 3123-3128.
- [32] R. Baharom, M. N. Seroji, M. K. M. Salleh, and I. M. Yassin, "Steady-state analysis of three-phase AC to DC converter using current injection hybrid resonant converter for power factor correction," in *Proc. 7<sup>th</sup> Int. Conf. on Intelligent Systems, Modelling and Simulation*, 2016, pp. 256-260.